

## A SIMPLE AND LOW-COST NEW PROCEDURE FOR SYNTHESIS OF NICKEL(II) AND CADMIUM(II) SULFIDES *in situ* THIOUREA METAL–CHELATION PRECURSOR

Moamen S. Refat<sup>1</sup>, Mohamed Y. El-Sayed<sup>2\*</sup>, Ibrahim H. Alsohaimi<sup>2</sup>, Hassan M. Hassan<sup>2</sup>,  
Thamer S. Alraddadid<sup>3</sup> and Sultan Akhtar<sup>4</sup>

<sup>1</sup>Department of Chemistry, College of Science, Taif University, P.O. Box 11099, Taif 21944, Saudi Arabia

<sup>2</sup>Chemistry Department, College of Science, Jouf University, P.O. Box: 2014, Sakaka, Saudi Arabia

<sup>3</sup>Department of Chemistry, College of Sciences and Arts-Alkamil, University of Jeddah, 23218, Jeddah, Saudi Arabia

<sup>4</sup>Department of Biophysics, Institute for Research and Medical Consultations, Imam Abdulrahman Bin Faisal University, Dammam, Saudi Arabia

(Received September 3, 2022; Revised November 30, 2022; Accepted November 30, 2022)

**ABSTRACT.** Nickel(II) and cadmium(II) sulfides are a promising chemical material in various advanced research areas such as solar cells, supercapacitors, catalysts, and of significant interest for their practical implementations in up to photonics and electronics. Cadmium and nickel sulfides were synthesized with stoichiometries in aqueous media at elevated temperature from  $\text{Ni}(\text{NO}_3)_2 \cdot 6\text{H}_2\text{O}$ ,  $\text{NiCl}_2 \cdot 6\text{H}_2\text{O}$ ,  $\text{NiSO}_4 \cdot 6\text{H}_2\text{O}$ ,  $\text{CdCl}_2$ ,  $\text{Cd}(\text{NO}_3)_2 \cdot 4\text{H}_2\text{O}$ ,  $\text{CdSO}_4 \cdot 8\text{H}_2\text{O}$  and thiourea as a sulfur precursor using a direct chemical reaction. At room temperature an octahedral and tetrahedral geometries result from the reactions between different nickel(II), cadmium(II) and thiourea with the molecular formulas can be presented as  $[\text{Ni}(\text{NH}_2\text{CSNH}_2)_6]\text{X}_2$  and  $[\text{Cd}(\text{NH}_2\text{CSNH}_2)_4]\text{X}_2$  where  $\text{X} = \text{Cl}^-$ ,  $\text{NO}_3^-$ ,  $\text{SO}_4^{2-}$ . The novelty of our study is precipitated yellow cadmium sulfide and black nickel sulfide at elevated temperature  $\sim 80^\circ\text{C}$  through the molar ratio 1:10 ( $\text{M}^{2+}$ : thiourea) in aqueous media. Infrared spectra, XRD, TEM including EDX, and elemental analysis were used for characterization the metal sulfides products. The average crystalline size of obtained CdS and NiS particles in range 20-25 nm. Different reaction conditions effects were evaluated on the size, morphology and particle size.

**KEY WORDS:** Nickel and cadmium sulfide, Chelation, Thiourea, XRD, TEM

## INTRODUCTION

Nickel sulfides were broadly investigated as one of metal sulfides owing to their different stoichiometries and phases and, ranging from the nickel-rich compound  $\text{Ni}_6\text{S}_5$ ,  $\text{Ni}_9\text{S}_8$ ,  $\text{Ni}_3\text{S}_2$ ,  $\text{NiS}$   $\text{Ni}_7\text{S}_6$ , are the sulfur rich compound like nickel disulfide and  $\text{Ni}_3\text{S}_4$  [1, 2]. NiS present in two main phases, at high temperatures  $\alpha$ -NiS hexagonal form is more stable, and at decreased temperatures the  $\beta$ -NiS rhombohedral form is stable [3]. Recently there are many applications for NiS, such as counter electrodes for solar cells [4] and the material for supercapacitors [5, 6] and lithium batteries electrodes [7, 8]. NiS is one of the metal sulfides which promising used in a wide range as cathode materials with high theoretical capacity for lithium batteries in hybrid vehicles [1]. Several approaches were recorded for the synthesis NiS by the synthesis from elements at raised temperature or the reaction solution of nickel(II) ions to sulfide ions [9]. Other techniques were reported for produce NiS, including mechanochemical [10], methods hydro/solvothermal [11], pyrolysis spray method [1], polyol method [3] decomposition of precursors by single-source [2, 12], synthesis by microwave [13] and preparation route in air by the solventless [14]. The NiS nanoparticles were prepared sonochemically in 2002 by Wang *et al.* [15] Through the effect of

\*Corresponding author. E-mail: [myelsayed@ju.edu.sa](mailto:myelsayed@ju.edu.sa) ; [iyosri@yahoo.com](mailto:iyosri@yahoo.com)

This work is licensed under the Creative Commons Attribution 4.0 International License

radiation on aqueous solution of  $\text{Ni}(\text{CH}_3\text{COO})_2$ ,  $\text{C}_2\text{H}_5\text{N}_5$  (TAA) and chelating agent triethanolamine. de la Parra-Arciniega *et al.* [16] have been used a new synthesis procedure for submicron particles of NiS using sonication of  $\text{Ni}(\text{NO}_3)_2$  solution containing TAA in various mixtures of ethanol and ionic liquid. In literature survey the cobalt sulfides have not been reported up to now by sonochemical synthesis, although of some other cobalt precursors nanocrystals, e.g.  $\text{Co}_3\text{O}_4$  [17]. The basic goal of this study was based on fruitfully fabrication of NiS and CdS NPs via simple cheap method. For this, different stoichiometric ratios aqueous solutions of sulfides and Ni, Cd were synthesized from their corresponding Chlorides, nitrate and sulphate. (CdS, CdSe, CdTe, etc.) Fluorescent nanoparticles have been used in conjugation with biomaterial such as polypeptides, nucleic acids, and antibodies, since these nanoparticles have fluorescent emission 20 times more effect than those fluoroprobes [18, 19]. These materials were used for improving the visualization of latent finger marks, or for frail fingerprints [19]. In the last years NPs CdS have been applied for their diverse electronic [20-22] catalytic application [22] and have optical [23-26] properties more than the normal forms [27]. CdS nanoparticles is effectively applied in medicine, facilitate diagnosis and treatment of cancer [28]. CdS were utilized for cancer imaging, we use ultraviolet radiation to activate nanoparticles accumulated inside target cancer cells can be easily visualized [29]. Fluorescent nanoparticles can be photoactivated (photodynamic) can be used for cancer therapy, cell death in accumulated cells catalyzed by the effect of radio sensitizing agents [30]. There are various techniques were applied for the preparation of nanoparticles CdS that commonly comprises chemicals, some conditions such as high pressure, and temperature. Recently, the biological synthesis is considered simpler method for metal nanoparticles synthesis [31] it needs milder conditions for the fabrication. CdS nanoparticles preparation from bacteria had previously been reported [28, 32], fungi [35] and yeast [33]. Lester *et al.* have been discovered that *Brevibacterium sp.* is one of the most organisms' that resistant to heavy metal ions inhibition [34]. The uptake of Cd by *Brevibacterium* was about of  $140 \text{ mmol kg}^{-1}$  recorded by Huang *et al.* [35]. CdS n-type semiconductor is a direct band gap of 2.4 eV. Quantum dot-sensitized solar cells based on use cadmium sulfide. It also used in nonlinear optics applications [36], light-emitting diodes [37], solar energy conversion [38], transistors thin film [39], gas detectors [40], optoelectronics [41], photo catalysis [42], photovoltaic cells, detectors of X-ray [43] it has high absorption coefficient so that it is utilized as a window compound for hetero-junction solar cells [44]. This article aims to manufacture nickel-cadmium sulfide in a simple and low-cost manner. The compounding agent method which applied to prepare nanoparticles of sulfides has many advantages when compared to other method used: low reaction time, high product yield and easy control. The synthesis process was done without used any toxic precursors and organic solvents but were performed in aqueous solution as a green chemistry research.

## EXPERIMENTAL

### *Synthesis*

The chemicals used herein in this article are in high grade and used without any further purifications. Precursors of both cadmium and nickel,  $\text{Ni}(\text{NO}_3)_2 \cdot 6\text{H}_2\text{O}$ ,  $\text{NiCl}_2 \cdot 6\text{H}_2\text{O}$ ,  $\text{NiSO}_4 \cdot 6\text{H}_2\text{O}$ ,  $\text{CdCl}_2$ ,  $\text{Cd}(\text{NO}_3)_2 \cdot 4\text{H}_2\text{O}$ ,  $\text{CdSO}_4 \cdot 8\text{H}_2\text{O}$ , and thiourea,  $\text{CH}_4\text{N}_2\text{S}$  were obtained from Sigma-Aldrich. The solid six samples were synthesized as, the dissolving thiourea (7.70 g, 100 mmol) in deionized water (100 mL) in volumetric flask 250 mL. Then adding 10 mmol of dissolved/suspended of  $\text{Ni}(\text{NO}_3)_2 \cdot 6\text{H}_2\text{O}$ ,  $\text{NiCl}_2 \cdot 6\text{H}_2\text{O}$ ,  $\text{NiSO}_4 \cdot 6\text{H}_2\text{O}$ ,  $\text{CdCl}_2$ ,  $\text{Cd}(\text{NO}_3)_2 \cdot 4\text{H}_2\text{O}$ ,  $\text{CdSO}_4 \cdot 8\text{H}_2\text{O}$  in 10 mL water. Heating the resulting mixtures under reflux for 24 h. The yellow and black precipitations of cadmium sulfide and nickel sulfide compounds were separated and rinsed many times with warm water then dried at  $90^\circ\text{C}$  in an oven for 3 h. The products yields were in ratio 70-76%.

### Apparatus

The elemental analysis was performed using a CHN 2400 Perkin Elmer. The percentage of nickel and cadmium in the compound's solutions were estimated by using atomic absorption method. A spectrometer model PYE-UNICAM SP 1900 fitted with the corresponding lamp was used for this purpose. The infrared spectra were recorded on the IR Affinity-IS Shimadzu FT-IR spectrophotometer (4000 – 400  $\text{cm}^{-1}$ ). XRD pattern of the adsorbent was measured using CuK $\alpha$  radiation by Shimadzu X-Ray powder diffractometer (XRD 7000) within  $2\theta$  ranging from 10 to 80°. TEM images were scanned based on the JEOL 100s microscopy.

## RESULTS AND DISCUSSION

### Preface on metal–thiourea complexes

A few metal complexes of thiourea were reported [45]. The first metals studied (platinum, palladium, zinc, and nickel) form metal-S bonds, since increase stretching frequency of C-N bond and decreases stretching frequency of the C-S bond upon coordination without an appreciable change stretching frequency of the  $\nu(\text{NH})$ . Using the same explanation, complexes of thiourea as chelating agent with  $\text{Fe}^{+2}$ ,  $\text{Mn}^{+2}$ ,  $\text{Co}^{+2}$ ,  $\text{Cu}^{+1}$ ,  $\text{Hg}^{+2}$ ,  $\text{Cd}^{+2}$ , and  $\text{Pb}^{+2}$  were also shown to be S-bonded modes [46]. But N-bonded reported only for titanium(IV) thiourea complex [47]. The compounds of thiocarbamide  $\text{H}_2\text{NCSNH}_2$   $[\text{Ni}(\text{tu})_6]\text{X}_2$  (where tu = thiourea and X =  $\text{BF}_4$ ,  $\text{ClO}_4$ , nitrate),  $[\text{Ni}(\text{tu})_2\text{X}_2]_n$  (known that X =  $\text{NO}_3$ , perchlorate), the square planar  $[\text{Ni}(\text{tu})_4]\text{X}_2$  (where X =  $\frac{1}{2}\text{SO}_4$ , fluoride) and the compound formed in dimethylformamide solution  $[\text{Ni}(\text{tu})_3(\text{DMF})\text{SO}_4]\cdot\text{DMF}$ , their structures discussed and described. The prepared six coordinated complexes  $[\text{Ni}(\text{tu})_2\text{X}_2]_n$  (X = nitrate,  $\text{ClO}_4$ ) have thiourea as bridging ligands. The formed species  $[\text{Ni}(\text{tu})_4]^{2+}$  is in acetone solutions of the complexes  $[\text{Ni}(\text{tu})_6]\text{X}_2$  (X =  $\text{BF}_4$ ,  $\text{ClO}_4$ ). The explained geometry is based on measurement spectral data (UV and IR), magnetic and conductivity [47]. The integration between  $^{113}\text{Cd}$  NMR and X-ray absorption spectroscopy were used for study the complexes developed in alcoholic solutions of cadmium salt with selenourea (SeU) or thiourea (TU), for thiourea also in aqueous medium. At decreased temperature, distinct signals  $^{113}\text{Cd}$  NMR were appeared, corresponding to  $[\text{CdL}_n]^{2+}$  species (where L = TU or SeU, n = 0–4) in which the ligand exchange is slow. For complexes of cadmium(II) with selone (C=Se) or thione (C=S) moieties have a coordination feature as  $\text{Cd}(\text{SeU})_4^{2+}$  and  $\text{Cd}(\text{TU})_4^{2+}$ , respectively [48]. Octahedral nickel(II)  $[\text{Ni}(\text{tu})_6]^{2+}$  and tetrahedral cadmium(II) thiourea complexes  $[\text{Cd}(\text{tu})_4]^{2+}$ , (tu = thiourea; Figure 1) has been previously synthesized and investigated [48].

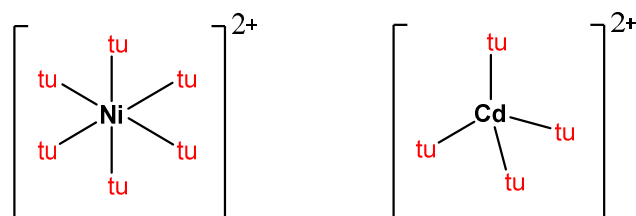
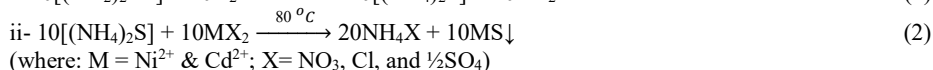
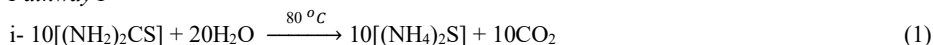


Figure 1. The octahedral Ni (II) and tetrahedral Cd (II) thiourea complex at room temperature.

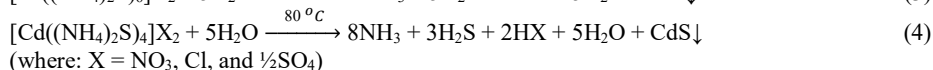
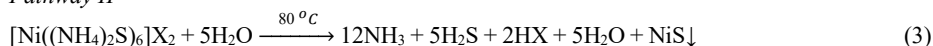
The chemical reactions between thiourea and  $(\text{Ni}(\text{NO}_3)_2 \cdot 6\text{H}_2\text{O}$ ,  $\text{NiCl}_2 \cdot 6\text{H}_2\text{O}$ ,  $\text{NiSO}_4 \cdot 6\text{H}_2\text{O}$ ,  $\text{CdCl}_2$ ,  $\text{Cd}(\text{NO}_3)_2 \cdot 4\text{H}_2\text{O}$ ,  $\text{CdSO}_4 \cdot 8\text{H}_2\text{O}$ ) inorganic salts by molar ratio 1:10 (metal(II) salt: thiourea) in aqueous solutions at  $\sim 80^\circ\text{C}$  formed a black (NiS) and yellow (CdS) solid precipitations for the

(Ni(NO<sub>3</sub>)<sub>2</sub>·6H<sub>2</sub>O, NiCl<sub>2</sub>·6H<sub>2</sub>O, NiSO<sub>4</sub>·6H<sub>2</sub>O) and (CdCl<sub>2</sub>, Cd(NO<sub>3</sub>)<sub>2</sub>·4H<sub>2</sub>O, CdSO<sub>4</sub>·8H<sub>2</sub>O) salts reacted with thiourea, respectively. In general, we can report the metal (Ni<sup>2+</sup>/Cd<sup>2+</sup>) ions main role as a catalyst for bond breaking in thiourea compound between sulfur and carbon atoms the following suggesting mechanism of reaction illustrated briefly as the following reaction mechanism for synthesis of NiS and CdS at ~80 °C:

*Pathway I*



*Pathway II*



Thus, in the above mechanism of reaction to form sulfides of nickel(II) and cadmium(II), in first step pathway hydrolyzed the thiourea by water molecules to form carbon dioxide and ammonium sulfide, which further reacted with metal ions in the second step to produce ammonium salts and sulfide metal compound. The second pathway was discussed the function of metal ions in the degradation of octahedral nickel(II) [Ni(tu)<sub>6</sub>]<sup>2+</sup> and tetrahedral cadmium(II) [Cd(tu)<sub>4</sub>]<sup>2+</sup> thiourea complexes in an aqueous media at ~80 °C. It is difficult to generalize the obtained result to all salts of transition metals, but we can say that metals and their various ions have an essential role in controlling the output of chemical reactions. This fact was confirmed in this paper where we found that nitrate, sulfate and chloride ions, all gave pure cadmium(II) yellow sulfide and nickel(II) black sulfide.

*Nickel(II) sulfide, NiS*

Figure 2 shows the Infrared spectra for the prepared nanoparticles of NiS. The band presence at 460 cm<sup>-1</sup> is broad can be attributed to sulfides, which is in good matching with IR results were recorded for nanosized NiS [3, 49]. The nickel sulfide has a different phase, like NiS<sub>2</sub> cubic, NiS hexagonal, Ni<sub>7</sub>S<sub>6</sub> orthorhombic, and Ni<sub>3</sub>S<sub>2</sub> trigonal, furthermore, sulfur resources were critical in the preparation of nickel sulfide class substances. The impact of solvents and reaction temperatures on the phase structure and precise composition of the end products was used to examine putative growth processes.

Figure 3 plots the X-ray diffraction pattern of the prepared NiS reported in the range of 2θ from 10° to 80° to emphasize its structure crystallography and purity of phases. Many diffraction peaks well-defined at 2θ = 79.17°, 73.68°, 71.97°, 65.34°, 64.39°, 62.68°, 60.98°, 52.64°, 45.25°, 35.39°, 33.69° and 31.06°, there are referred to the (104), (202), (004), (200), (103), (110), (102), (101), (002) and (100) planes α-NiS hexagonal (JCPDS No.: 75-0613, space group: P63/mmc, c = 5.30 Å, a = b = 3.42 Å). Also, the mean particle size of the product was calculated by the Scherer equation [49]:

$$D = 0.9\lambda/\beta\text{Cos}\theta \quad (5)$$

where θ is the peak position angle, λ is X-ray radiation wavelength and β is the width of appeared diffraction line at its half-maximum intensity. The results display that the mean crystal size of the prepared NiS particles in the range of 20–25 nm.

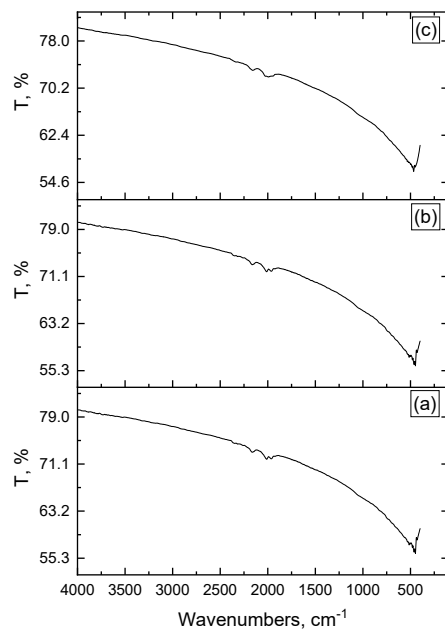


Figure 2. FTIR spectra of pure NiS NPs. Synthesized nickel sulfide nanoparticles by reaction of thiourea and (a)  $\text{Ni}(\text{NO}_3)_2$ , (b)  $\text{NiCl}_2$ , and (c)  $\text{NiSO}_4$ , respectively.

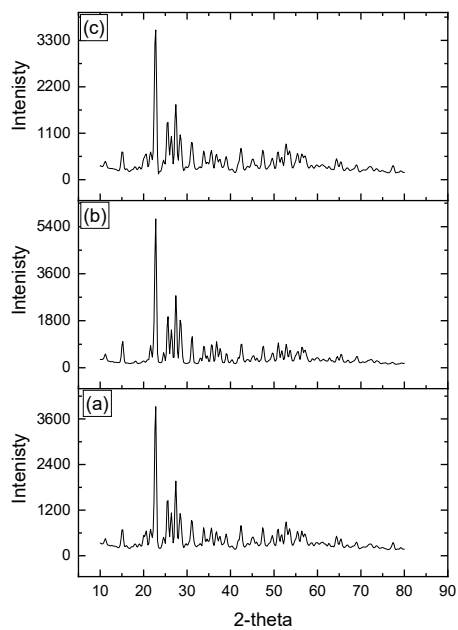


Figure 3. XRD profiles of pure NiS NPs. nickel sulfide nanoparticles were synthesized by reaction of thiourea and (a)  $\text{Ni}(\text{NO}_3)_2$ , (b)  $\text{NiCl}_2$ , and (c)  $\text{NiSO}_4$ , respectively.

In Figure 4 TEM micrograph shows spherical morphology of NiS is revealed clearly from the annular dark-field of high-angle scanning transmission electron microscope, which was showed as particles aggregated within the range diameters of 25-30 nm. The EDX spectrum shown in (Figure 4D) demonstrated the homogeneous distribution of S and Ni throughout the nanostructures NiS. Despite substantial agglomeration and a wide range of nanostructure sizes, the materials exhibit good crystallinity and phase purity.

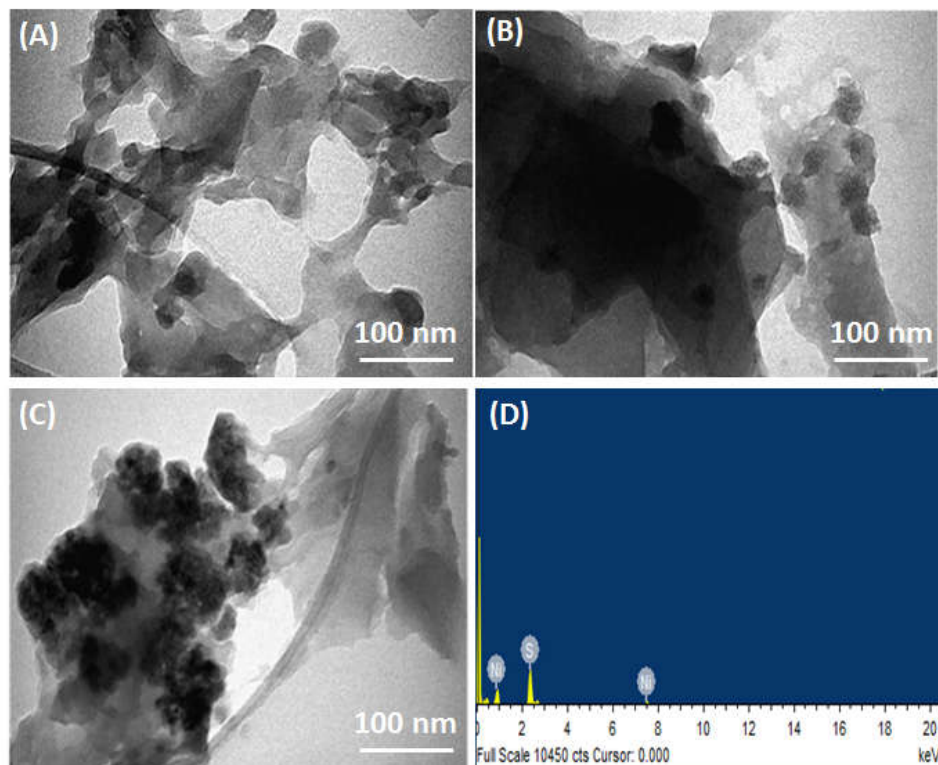


Figure 4. TEM images of pure NiS NPs were synthesized by reaction of thiourea and (A)  $\text{Ni}(\text{NO}_3)_2$ , (B)  $\text{NiCl}_2$ , and (C)  $\text{NiSO}_4$  respectively, and (D) EDX of as-synthesized NiS NPs.

#### *Cadmium(II) sulfide, CdS*

The infrared spectra of the synthesized nanoparticles cadmium sulfide is depicted in the Figure 5. The infrared spectra for CdS nanoparticles show stretching vibration peak at  $3691$  and  $3505\text{ cm}^{-1}$  ascribed to the O-H free moiety and the observed peak at  $1600\text{ cm}^{-1}$  is referred to hydroxyl group of  $\text{H}_2\text{O}$  and the bands at  $1056$  and  $1014\text{ cm}^{-1}$  related to S-O and the bands at  $650$  and  $514\text{ cm}^{-1}$  is assigned to presence S-S bond. The vibration band at  $438\text{ cm}^{-1}$  corresponding to Cd-S [40-42]. The particles of CdS have the average grain size range  $12\text{-}20\text{ nm}$ . The X-ray diffractogram of CdS nanoparticles are shown in Figure 6. A good matching results between the practical diffraction angle  $2\theta$  and the standard diffraction of specimen is evidence standard of the samples. Cadmium sulfide pattern has many distinguish peaks at  $2\theta$  values are shown and listed in (Table 1) and

compared with the card values of standard diffraction (JCPDS), CdS card No. 02-0563. Further to investigate the morphology of the prepared CdS NPs, TEM was performed. Images observed from the TEM analysis attributed to the synthesized nanoparticles were uniform morphology and spherical/rod in shape. The particles size ranged between 10-20 nm and the shape of these particles are appeared to be almost spherical/rods (Figure 7). To investigate the elemental composition of the prepared metal sulfides nanoparticles, EDX spectrum was measured. In the EDX spectrum appear strong bands from the NPs demonstrated the presence of S and Cd alone (Figure 7D) without the presence other contaminated atoms in the reaction mixture. These results proof that the synthesized NPs are generated of CdS only.

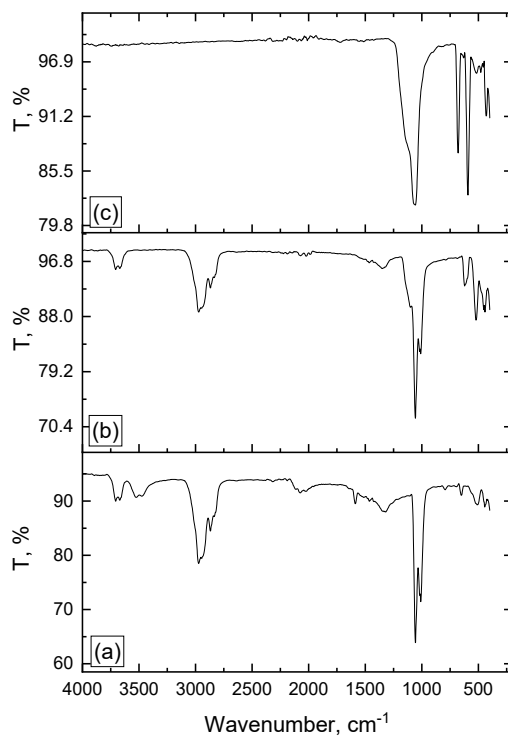


Figure 5. Infrared spectra of pure CdS NPs. Synthesized cadmium sulfide nanoparticles by reaction of thiourea and (a)  $\text{Cd}(\text{NO}_3)_2$ , (b)  $\text{CdCl}_2$ , and (c)  $\text{CdSO}_4$ , respectively.

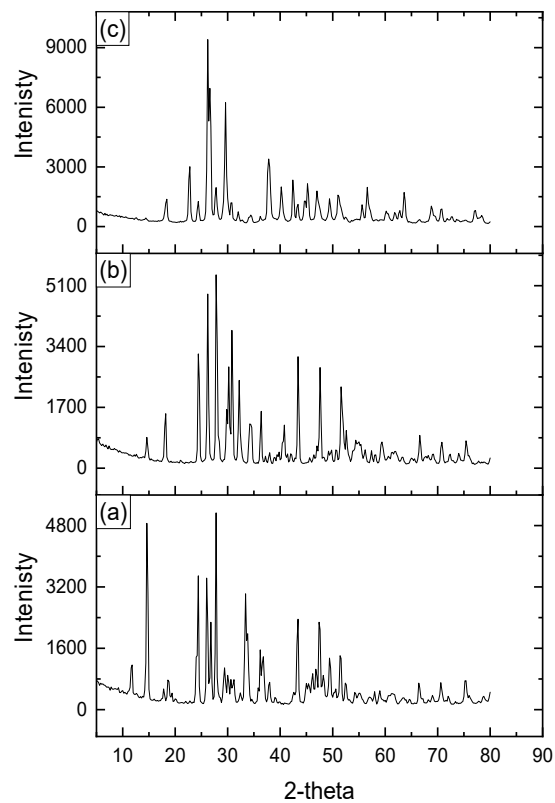


Figure 6. XRD spectrum of pure CdS NPs. Synthesized cadmium sulfide nanoparticles by reaction of thiourea and (a)  $\text{Cd}(\text{NO}_3)_2$ , (b)  $\text{CdCl}_2$ , and (c)  $\text{CdSO}_4$ , respectively.

Table 1. Practical and standard diffraction angles of synthesized CdS NPs.

Experimental CdS	Standard – JCPDS 02-0563
11.894	11.462
14.547	13.048
18.716	19.818
24.402	23.375
25.918	26.099
27.813	29.336
33.309	32.682
35.963	35.589
38.048	38.696
43.354	43.724
47.334	46.068
51.314	51.567

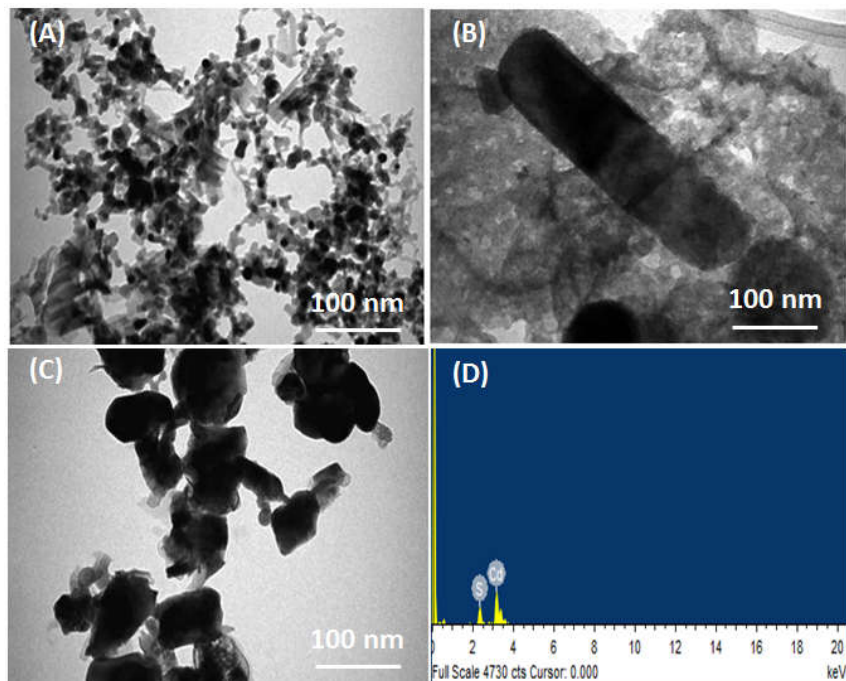


Figure 7. TEM images of CdS nanoparticles were synthesized by reaction of thiourea and (A)  $\text{Cd}(\text{NO}_3)_2$ , (B)  $\text{CdCl}_2$ , (C)  $\text{CdSO}_4$  respectively, and (D) EDX of as-synthesized CdS NPs.

## CONCLUSION

Metal sulfides are the most important group of ore minerals that constitute charge materials for most non-ferrous metal production processes worldwide. For example, nickel sulfide chemistry is used to solve associated environmental problems, such as the disposal of radioactive waste. Also, the cadmium sulfide is an important direct intermediate bandgap with excellent thermal and chemical stability and strong optical absorption, and is used in solar cells, light emitting diodes, and lasers. Therefore, in our article the nickel and cadmium sulfide nanoparticles have been prepared by simple and low-cost chemical approach. According to XRD measurements, the typical particle size is in the nano range (12–25 nm). The TEM image shows well-nanocrystalline particles with uniform shape. The stretching and bending frequencies of the sample's molecular functional groups are investigated using the FTIR spectrum.

## REFERENCES

1. Mondal, D.; Villemure, G.; Song, C. Synthesis, characterization, and evaluation of unsupported porous NiS submicrometer spheres as cathode material for lithium batteries. *J. Appl. Electrochem.* **2014**, *44*, 599–606.
2. Yin, P.F.; Sun, L.L.; Zhou, C.; Sun, Y.H.; Han, X.Y.; Deng, C.R. Characterization and magnetic property of 3D flower-like nickel sulphide nanocrystals through decomposing bis(thiourea) nickel(II) chloride crystals. *Bull. Mater. Sci.* **2015**, *38*, 95–99.

3. Surendran, S.; Sankar, K.V.; Berchmans, L.J.; Selvan, R.K. Polyol synthesis of  $\alpha$ -NiS particles and its physic-chemical properties. *Mater. Sci. Semicond. Process.* **2015**, *33*, 16–23.
4. Kim, H.J.; Yeo, T.B.; Kim, S.K.; Rao, S.S.; Savariraj, A.D.; Prabakar, K.; Chandu, V.M.G. Optimal-temperature-based highly efficient NiS counter electrode for quantum-dot-sensitized solar cells. *Eur. J. Inorg. Chem.* **2014**, *2014*, 4281–4286.
5. Sun, C.C.; Ma, M.Z.; Yang, J.; Zhang, Y.F.; Chen, P.; Huang, W.; Dong, X.C. Phase-controlled synthesis of  $\alpha$ -NiS nanoparticles confined in carbon nanorods for high performance supercapacitors. *Sci. Rep.* **2014**, *4*, 7054.
6. Chen, H.C.; Jiang, J.J.; Zhao, Y.D.; Zhang, L.; Guo, D.Q.; Xia, D.D. One-pot synthesis of porous nickel cobalt sulphides: tuning the composition for superior pseudocapacitance. *J. Mater. Chem. A* **2015**, *3*, 428–437.
7. Wang, Y.; Zhu, Q.S.; Tao, L.; Su, X.-W. Controlled synthesis of NiS hierarchical hollow microspheres with different building blocks and their application in lithium batteries. *J. Mater. Chem.* **2011**, *21*, 9248–9254.
8. Tao, H.-C.; Yang, X.-L.; Zhang, L.L.; Ni, S.B. One step synthesis of nickel sulfide/N-doped graphene composite as anode material for lithium-ion batteries. *J. Electroanal. Chem.* **2015**, *739*, 36–42.
9. Cotton, F.A.; Wilkinson, G. *Advanced Inorganic Chemistry*, 4th ed., John Wiley and Sons: New York; **1980**.
10. Kosmač, T.; Maurice, D.; Courtney, T.H. Synthesis of nickel sulfides by mechanical alloying, *J. Am. Ceram. Soc.* **1993**, *76*, 2345–2352.
11. Nagaveena, S.; Mahadevan, C.K. Preparation by a facile method and characterization of amorphous and crystalline nickel sulfide nanophases. *J. Alloys Compd.* **2014**, *582*, 447–456.
12. Yin, P.F.; Zhou, C.; Han, X.Y.; Zhang, Z. R.; Xia, C.H.; Sun, L.L. Shape and phase evolution of nickel sulfide nano/microcrystallines via a facile way. *J. Alloys Compd.* **2015**, *620*, 42–47.
13. Salavati-Niasari, M.; Banaiean-Monafred, G.; Emadi, H.; Enhessari, M. Synthesis and characterization of nickel sulfide nanoparticles via cyclic microwave radiation. *C.R. Chim.* **2013**, *16*, 929–936.
14. Schmachtenberg, V.A.V.; Tontini, G.; Koch, J.A.; Semione, G.D.L.; Drago, V. Low temperature solventless syntheses of nanocrystalline nickel sulfides with different sulfur sources. *J. Phys. Chem. Solids.* **2015**, *87*, 253–258.
15. Wang H.; Zhang, J.R.; Zhang, X. N.; Zhao, S. X.; Zhu, J.J. Preparation of copper monosulfide and nickel monosulfide nanoparticles by sonochemical method. *Mater. Lett.* **2002**, *55*, 253–258.
16. de la Parra-Arciniega, S.M.; García-Gómez, N.A.; Garcia-Gutierrez, D.I.; Salinas-Estevané, P.; Sánchez, E.M. Ionic liquid assisted sonochemical synthesis of NiS submicron particles. *Mater. Sci. Semicond. Process.* **2014**, *23*, 7–13.
17. Askarinejad, A.; Morsali, A. Direct ultrasonic-assisted synthesis of sphere-like nanocrystals of spinel  $\text{Co}_3\text{O}_4$  and  $\text{Mn}_3\text{O}_4$ . *Ultrason. Sonochem.* **2009**, *16*, 124–131.
18. Smith, A.M.; Gao, X.; Nie S. Quantum dot nanocrystals for in vivo molecular and cellular imaging. *Photochem. Photobiol.* **2004**, *80*, 377–385.
19. Jamieson, T.; Bakhshi, R.; Petrova, D.; Pockock, R.; Imani, M.; Seifalian, AM. Biological applications of quantum dots. *Biomaterials* **2007**, *28*, 4717–4732.
20. Smith, A.M.; Duan, H.; Mohs, A.M.; Nie, S. Bioconjugated quantum dots for in vivo molecular and cellular imaging. *Adv. Drug Deliv. Rev.* **2008**, *60*, 1226–1240.
21. Hu, J.; Odom, T.W.; Lieber, C.M. Chemistry and physics in one dimension: synthesis and properties of nanowires and nanotubes. *Acc. Chem. Res.* **1999**, *32*, 435–445.
22. Sweeney, R.Y.; Mao, C.; Gao, X.; Burt, J.L.; Belcher, A.M.; Georgiou, G. Bacterial biosynthesis of cadmium sulfide nanocrystals. *Chem. Biol.* **2004**, *11*, 1553–1559.
23. Krolkowska, A.; Kudelski, A.; Michota, A.; Bukowski, J. SERS studies on the structure of thioglycolic acid monolayers on silver and gold. *Surf. Sci.* **2003**, *532*, 227–232.

24. Mohanpurta, P.; Rana, N.K.; Yadav, S.K. Biosynthesis of nanoparticles: technological concepts and future applications. *J. Nanopart. Res.* **2007**, *9*, 1165–1170.
25. Mandal, D.; Bolander, M.E.; Mukhopadhyay, D.; Sarkar, G.; Mukherjee, P. The use of microorganisms for the formation of metal nanoparticles and their applications. *Appl. Microbiol. Biotechnol.* **2006**, *69*, 485–492.
26. Murray, C.B.; Kagan, C.R.; Bawendi, M.G. Synthesis and characterization of monodisperse nanocrystals and close-packed nanocrystal assemblies. *Annu. Rev. Mater. Sci.* **2000**, *30*, 545–610.
27. Shankar, S.S.; Ahmad, A.; Sastry, M. Geranium leaf assisted biosynthesis of silver nanoparticles. *Biotechnol. Prog.* **2003**, *19*, 1627–1631.
28. Biju, V.; Itoh, T.; Ishikawa, M. Delivering quantum dots to cells: bioconjugated quantum dots for targeted and nonspecific extracellular and intracellular imaging. *Chem. Soc. Rev.* **2010**, *39*, 3031–3056.
29. Akerman, M.E.; Chan, W.C.W.; Laaskonen, P.; Bhatia, S.N.; Ruoslahti, E. Nanocrystal targeting in vivo. *Proc. Natl. Acad. Sci. USA* **2002**, *99*, 12617–12621.
30. Juzenas, P.; Chen, W.; Sun, Y.P.; Coelho, M.A.N. Genralov, R.; Genralova, N. Quantum dots and nanoparticles for photodynamic and radiation therapies of cancer. *Adv. Drug. Deliv. Rev.* **2008**, *60*, 1600–1614.
31. Kalishwaralal, K.; Deepak, V.; Pandian, S.R.K. Kottaisamy, M.; Barath, M.K.S.; Kartikeyan, B. Biosynthesis of silver and gold nanoparticles using *Brevibacterium casei*. *Colloids Surf. B* **2010**, *77*, 257–262.
32. Bai, H.; Zhang, Z.; Guo, Y.; Jia, W. Biological synthesis of size-controlled cadmium sulfide nanoparticles using immobilized *Rhodobacter sphaeroides*. *Nanoscale Res. Lett.* **2009**, *4*, 717–723.
33. Kowshik, M.; Deshmukh, N.; Vogel, W.; Urban, J.; Kulkarni, S.K.; Paknikar, K.M. Microbial synthesis of semiconductor CdS nanoparticles, their characterization, and their use in the fabrication of an ideal diode. *Biotechnol. Bioeng.* **2002**, *78*, 583–588.
34. Lester, J.N.; Perry, R.; Dadd, A.H. The influence of heavy metals in a mixed population of sewage origin in the chemostat. *Water Res.* **1979**, *13*, 1055–1063.
35. Huang, Q.; Chen, W.; Xu, L. Adsorption of copper and cadmium by Cu- and Cd-resistant bacteria and their composites with soil colloids and kaolinite. *Geomicrobiol. J.* **2005**, *22*, 227–236.
36. Liu, Y.K.; Zapien J.A.; Geng, C.Y.; Shan, Y.Y.; Lee, C.S.; Lifshitz, Y.; Lee, S.T. High-quality CdS nanoribbons with lasing cavity. *Appl. Phys. Lett.* **2004**, *85*, 3241–3243.
37. Gopal, A.; Hoshino, K.; Kim, S.; Zhang, X. Multi-color colloidal quantum dot-based light emitting diodes micropatterned on silicon hole transporting layers. *Nano Technol.* **2009**, *20*, 235201.
38. Weller, H. Synthesis and self-assembly of colloidal nanoparticles. *Philos. Trans. R Soc. A Math. Phys. Eng. Sci.* **2003**, *361*, 229–240
39. Duan, X.; Huang, F.Y.; Agarwal, R.; Lieber, C.M. Single-nanowire electrically driven lasers. *Nature.* **2003**, *421*, 241–245.
40. Afify, H.H.; Battisha, I.K. Oxygen interaction with CdS based gas sensors by varying different preparation parameters. *J. Mater. Sci. Mater. Electron.* **2000**, *11*, 373–377.
41. Hikmet, R.A.M.; Talapin, V.; Weller, H. Study of conduction mechanism and electroluminescence in CdS/ZnS quantum dot composites. *J. Appl. Phys.* **2003**, *93*, 3509–3514.
42. Huynh, W.V.; Dittmer, J.J.; Alivisatos, A.P. Hybrid nanorod– polymer solar cells. *Science.* **2002**, *295*, 2425–2427.
43. Frerichs, R. The cadmium sulfide X-ray detector. *J. Appl. Phys.* **1950**, *21*, 312–317.

44. Oladeji, I.O.; Chow, L.; Ferekides, C.S.; Viswanathan, V.; Zhao, Z. Metal/CdTe/CdS/Cd<sub>1-x</sub>ZnxS/TCO/glass: a new CdTe thin film solar cell structure. *Sol. Energy Mater. Sol. Cells.* **2000**, *61*, 203–211.
45. Yamaguchi, A.; Penland, R.B.; Mizushima, S.; Lane, T.J.; Columba, C; Quagliano, J.V. Infrared absorption spectra of inorganic coordination complexes. XIV. Infrared studies of some metal thiourea complexes. *J. Amer. Chem. Soc.* **1958**, *80*, 527–529.
46. Bailey, R.A.; Peterson T.R. Some complexes of Fe(II) with thiourea ligands. *J. Chem.* **1967**, *45*, 1135–1142.
47. Rivest, R. Coordination complexes of titanium(IV) halides: III. Preparation and infrared spectra of the complexes of titanium tetrachloride with urea, thiourea, and some of their derivatives. *Canad. J. Chem.* **1962**, *40*, 2234–2242.
48. Basso, S.; Costamagna, J.A.; Levitus, R. Complexes of some nickel(II) salts with thiourea. *J. Inorg. Nucl. Chem.* **1969**, *31*, 1797–1805.
49. Fazli Y.; Pourmortazavi, S.M.; Kohsari, I.; Sadeghpur, M. Electrochemical synthesis and structure characterization of nickel sulfide nanoparticles. *Mater. Sci. Semicond. Process.* **2014**, *27* 362–367.